

OPACITY PROJECT: AN OVERVIEW AND SOME PRELIMINARY RESULTS

(Invited Talk)

C. Mendoza

IBM Venezuela Scientific Center

RESUMEN. El *Proyecto de la Opacidad* es un esfuerzo internacional dedicado a calcular con precisión la gran cantidad de datos atómicos que se necesitan para estimar opacidades en los envoltentes estelares. Describimos el panorama general del proyecto incluyendo aspectos astrofísicos, físico-atómicos y computacionales. El volumen y calidad de los datos que se están generando se puede apreciar en los resultados preliminares que se presentan.

ABSTRACT. The *Opacity Project* is an international effort dedicated to the calculation of the vast, accurate, atomic data required to estimate stellar envelope opacities. We give an overview of the project including astrophysical, atomic-physical and computational aspects. The volume and quality of the data which are being generated can be appreciated in the preliminary results that are presented.

Key words: ATOMIC PROCESSES – OPACITIES – STARS-INTERIORS

I. INTRODUCTION

A large collaborative effort, usually referred to as the *Opacity Project* (OP), was started about six years ago aimed at accurately calculating the extensive atomic data that are required to estimate stellar envelope opacities. It has involved research groups from France, Germany, the United Kingdom, USA and Venezuela. Although we need not emphasise the importance of reliable opacity values in several research fields, the main incentive that led to the launching of the project arose from long-standing problems in the quantitative description of pulsating stars, particularly the Classical Cepheids (Cox 1980, Simon 1982). The OP is currently well advanced: most of the atomic data for astrophysically abundant elements from H to Fe has been calculated (the series of papers “Atomic data for opacity calculations”, Seaton 1987a and contributions thereafter); an improved *equation of state* (EOS) has been developed (the series “The equation of state for stellar envelopes”, Hummer and Mihalas 1988 and papers thereafter) and mean opacities for single elements and mixtures are now being calculated.

In the present talk we attempt to give a comprehensive survey of the project and therefore discussions will be kept at an informal level. In section II we introduce the *Rosseland mean opacity* (RMO) in the context of radiative transfer processes in the stellar envelope. The *mass problem* of Classical Cepheids is discussed in section III in connection with a suggested revision of metal opacities. Previous opacity calculations are briefly reviewed in section IV. The OP is described in section V, including the methods employed to compute the atomic data, the main features of the proposed EOS and the approach to treat *line broadening*. In section VI we have selected the Mg isoelectronic sequence to give a general feeling for the volume and accuracy of the atomic data that are being produced.

II. STELLAR ENVELOPE OPACITIES

2.1. Equation of radiative transfer

Radiative flow in a plasma is usually described by the equation

$$\frac{dI_\nu}{ds} = -\kappa'_\nu I_\nu + j_\nu \quad (1)$$

where $I_\nu \equiv I(\mathbf{r}, \hat{\mathbf{n}}, \nu, t)$ is the *specific intensity* of the beam at a point \mathbf{r} traveling in a direction $\hat{\mathbf{n}}$, and ds is a length element in the same direction. I_ν is defined such that the energy passing through a surface element dS (here assumed to be perpendicular to the beam direction) by radiation of frequency $(\nu, \nu + d\nu)$ into a solid angle $d\Omega$ during a time interval dt is given by

$$\delta E = I_\nu dS d\Omega d\nu dt . \quad (2)$$

The parameters κ'_ν and j_ν are the *monochromatic opacity* and *emissivity* respectively; they determine the radiative absorption and emission characteristics of the plasma, and they depend on the plasma properties and on the radiation field itself. However, in thermodynamic equilibrium (TE) there is a simple relationship between κ'_ν and j_ν , namely *Kirchhoff's law*

$$j_\nu = \kappa'_\nu I_\nu \quad (\text{TE}) , \quad (3)$$

where I_ν now depends only on temperature and is given by the *Planck function*

$$I_\nu \equiv B_\nu(T) = (2h\nu^3/c^2) [\exp(h\nu/kT) - 1]^{-1} \quad (\text{TE}) . \quad (4)$$

In general the monochromatic opacity κ'_ν includes contributions from all radiative absorption processes in the plasma, and it must be corrected for *stimulated emission* which gives a negative contribution. In TE this correction takes the form

$$\kappa'_\nu = \kappa_\nu [1 - \exp(-h\nu/kT)] \quad (\text{TE}) , \quad (5)$$

where κ_ν is the *uncorrected monochromatic opacity*.

2.2. The Rosseland mean opacity (RMO)

In stellar envelopes, with typical temperature (K) and density (g/cm³) ranges of

$$4.5 \leq \log(T) \leq 6.5 \quad \text{and} \quad -8.5 \leq \log(\rho) \leq -1.5 , \quad (6)$$

local thermodynamic equilibrium (LTE) can be assumed. This means that the specific intensity of the radiation is not very different from the Planck function, and the radiative transport process can be approximated by a diffusion approximation (Mihalas 1978), whereby the total radiant energy flux is taken to be proportional to the temperature gradient:

$$\mathbf{F} = - \left(\frac{4\pi}{3\kappa_R} \frac{dB}{dT} \right) \nabla T \quad (\text{LTE}) \quad (7)$$

with

$$\frac{dB}{dT} = \int_0^\infty \frac{\partial B_\nu}{\partial T} d\nu \quad \text{and} \quad \frac{1}{\kappa_R} = \left[\int_0^\infty \frac{1}{\kappa'_\nu} \frac{\partial B_\nu}{\partial T} d\nu \right] \left[\frac{dB}{dT} \right]^{-1} . \quad (8)$$

Radiative transfer is now controlled by κ_R , the RMO, which can be expressed in terms of the uncorrected monochromatic opacity by the integral

$$\frac{1}{\kappa_R} = \int_0^\infty \frac{1}{\kappa_\nu} \times g(u) du , \quad (9)$$

where $g(u)$ is a weighting function (see fig. 1) given in terms of the reduced photon energy $u \equiv h\nu/kT$ by

$$g(u) = \frac{15}{4\pi^4} u^4 \exp(-u) [1 - \exp(-u)]^{-3} . \quad (10)$$

In the calculation of the RMO important considerations must be taken into account. The RMO is a weighted harmonic mean and consequently it is not additive; that is, all contributions to the monochromatic opacity must be determined before the integral in equation (9) is computed. The RMO weights the “windows” between absorption lines rather than the strong absorption lines themselves; therefore, accurate representations must be considered for the line wings, the weak lines and absorption lines arising from minor constituents of the plasma.

Seaton (1987a) has shown that, in the physical conditions of stellar envelopes, the average particle separation is greater than the ionic radii, and that transitions in ions with bound electrons give rise to substantial contributions to the opacity. Therefore the computation of envelope opacities lies mainly in the domain of atomic physics. The following atomic processes must be considered: bound-bound transitions (b-b); bound-free transitions (b-f); free-free transitions (f-f); line broadening mechanisms and scattering processes (e.g., Thomson

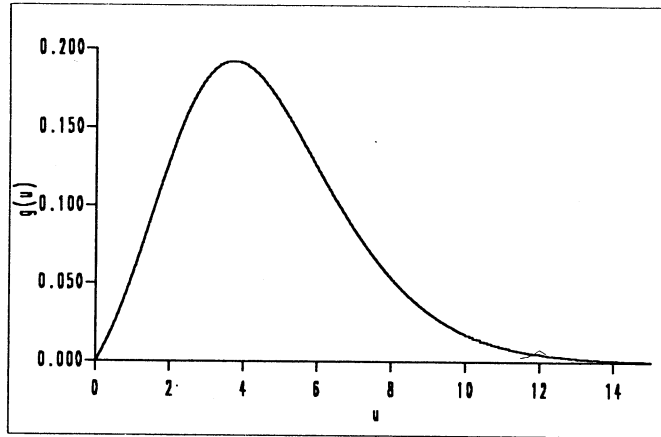


Figure 1. The Rosseland mean opacity weighting function $g(u)$ (see equation 10).

scattering). In particular, b-b and b-f transitions arising from both the ground and excited states must be included. The ionisation fractions and occupation numbers, which depend upon the thermodynamic properties of the plasma, are obtained by solving an EOS.

III. THE CEPHEID MASS PROBLEM

Classical Cepheids (Type I Cepheids) are bright pulsating stars which are grouped in a narrow, steep strip in the HR diagram (see fig. 2). They belong to Population I with periods, masses and radii in the ranges: $1^d \leq P \leq 70^d$; $3M_{\odot} \leq M \leq 16M_{\odot}$ and $10R_{\odot} \leq R \leq 150R_{\odot}$. Due to their intrinsic period-luminosity relation, they have been used as important galactic and extragalactic distance indicators (Feast and Walker 1987). Furthermore, Cepheids are fundamental test-cases in stellar evolution and pulsation theories. In this

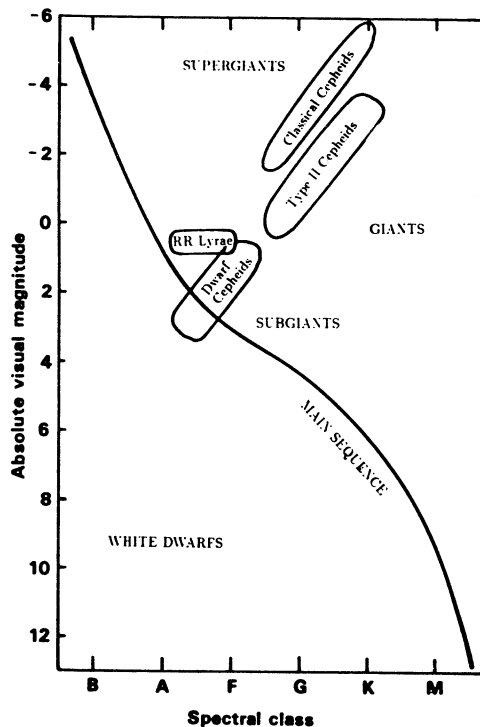


Figure 2. HR diagram showing the position of Classical Cepheids in relation to the main sequence and other pulsating stars.

respect, these two theoretical frameworks address different regions of the star: stellar evolution depends mainly on properties of the core whilst pulsations are believed to be due to ionisation mechanisms, particularly involving He II, at critical depths in the envelope.

From the evolutionary point of view, Classical Cepheids are stars in the post-main sequence stages where helium is being burned in the core. The well defined strip in the HR diagram containing these stars, as well as other pulsating stars such as the Type II Cepheids, the RR Lyrae and the dwarf Cepheids (see fig. 2), is known as the *instability strip* (Iben 1974). Evolutionary models (see, for instance, Becker 1985, 1987) show that intermediate-mass stars, as they leave the main sequence, can cross the instability strip one or several times. On the other hand, linear and non-linear pulsation models attempt to reproduce the star characteristic curves (light curve, radial and radial-velocity variations), its fundamental frequency and overtones. Understanding of the actual pulsation mechanisms should lead to explanations of the properties of the instability strip (e.g., its blue and red edges) and pulsating star properties such as the period-mean density and period-luminosity relations (Cox 1985). Finer details and peculiarities of light curves have also been studied; for instance, the bumps found in intermediate-period variables (the *bump Cepheids*) and modulations caused by double-mode behaviour in the *beat Cepheids* (Balona 1985).

In spite of sound qualitative agreement in predictions from both theories, on a quantitative level there remain standing discrepancies. Of much concern have been definite differences in the Cepheid masses predicted from evolutionary tracks and pulsational properties, namely $M_{evol} > M_{puls}$. Although Cox (1980) asserts that the mayor mass problem has been removed by the increased Hyades distance and by lower Cepheid temperatures, smaller Cepheid distances estimated more recently (e.g., Schmidt 1984) have kept the problem open. Moreover, persistently lower pulsational masses for the beat and bump Cepheids are still unsolved (Simon 1987).

Many suggestions have been put forward to eliminate the Cepheid mass anomaly: inclusion of mass loss in models; He enrichment in the outer layers; magnetic effects and errors in the model input physics, in particular poor opacity values. In this respect, several authors have advocated revisions of the existing opacities. For instance, Fricke *et al* (1971), in a study of the roles played by opacities in both evolutionary and pulsation models, have shown that the mass differences can be reduced by arbitrary changes in the interior and envelope opacities; Stellingwerf (1978) suggested an artificial opacity increase at 10^5 K to produce the β Cephei instability and Bertelli *et al* (1984) have found that discrepancies between theory and observations in galactic supergiants can be removed by a combination of effects including a moderate increase in the opacities for C, N and O. Perhaps the most influential proposal has been that due to Simon (1982), who has shown that an increase of a factor of 2 or 3 in the opacities for metals (elements heavier than He) would bring together the mass estimates obtained from the different methods, including those for the beat and bump Cepheids. In support for this revision of metal opacities, he argues that the mass problem does not arise in metal-poor variables such as the RR Lyrae and he criticises the methods that have been used to compute the atomic data for the heavier elements. Simon's point of view did influence some members of the atomic physics community who have undertaken revisions, and in the case of the OP it led to a major recalculation.

IV. PREVIOUS OPACITY CALCULATIONS

Previous work on opacities has been reviewed by Cox (1965), Carson (1976) and Huebner (1986). In this section we only give a brief summary of the more recent calculations.

4.1. Los Alamos Astrophysical Opacity Library (LAAOL)

Regarded at present as the standard opacities, the LAAOL emerged as a result of pioneering work by Cox *et al* (1965) and Cox and Stewart (1965, 1970a, b). Although originally based on hydrogenic methods (Cox 1965), results have been steadily refined keeping up to date with improvements in the atomic physics (Magee *et al* 1975, Cox and Tabor 1976). The proposal by Simon (1982) led to a revision of the metal contribution by Magee *et al* (1984), who concluded that a better treatment of the atomic data for the heavier ions would not result in the expected increases.

4.2. Carson Opacities

After a critical examination of the hydrogenic approximation by Carson and Hollingsworth (1968), Carson *et al* (1968) calculated astrophysical opacities using a Thomas-Fermi atomic model. They obtained large increases (factor of 10 at 10^6 K) for C, N, O (the so called "CNO bump"), Fe and a factor of ~ 2 for the critical second ionisation of He. The larger opacities encouraged authors to revisit problems in pulsation theory; for

instance, Vemury and Stothers (1978) obtained normal masses for bump Cepheids, and improved treatments of Type II Cepheids and long-period Cepheids were presented by Carson *et al* (1981) and Carson and Stothers (1984) respectively. However, in a comparative study with the LAAOL, Carson *et al* (1984) found that the Carson code was giving overestimated opacities, particularly the CNO bump, due to incorrect occupations of the $2p$ and higher levels for highly ionised metals. After this correction the two sets of results were found to be in satisfactory agreement.

4.3. Livermore Opacities

Also encouraged by Simon (1982), Iglesias *et al* (1987) have published a short report on a re-examination of metal opacities. In this work parametric potentials are employed to calculate the atomic data and a refined EOS formalism is introduced. The improved treatment of the atomic physics leads to significantly larger RMO in the density and temperature regimes important to Cepheid models.

V. OPACITY PROJECT

The main objective of the OP is to compute RMO for envelope conditions making use of accurate atomic data. Other mean opacities, such as the *Planck mean*, will also be considered. An opacity library for single chemical elements and their mixtures will be the end-product available to users. Important spinoffs from the project are an extensive atomic database and highly efficient computer packages that can be employed to solve definitively other atomic physics problems such as radiative recombination and electron-ion excitation. The general scope of the OP has been described previously by Seaton (1987a) and Pradhan (1987).

5.1. Close-coupling approximation

An important feature of the OP is that wave functions for ionic states, whether bound or free, are calculated within the same theoretical framework, namely the *close-coupling* (CC) method of electron-atom collision theory (Burke and Seaton 1971). Thus, photoexcitation and photoionisation can be treated with consistency in a unified approach that can be geared up for production of large amounts of data. Series perturbations and resonances, which strongly affect radiative processes, are taken into account in detail.

The wave function for a system consisting of an electron in the field of an N -electron ion is expanded in terms of the ion eigenfunctions:

$$\Psi^{SL\pi} = \mathcal{A} \sum_{i=1}^I \chi_i \frac{1}{r} F_i(r) + \sum_{j=1}^J c_j \Phi_j. \quad (11)$$

The ion is usually referred to as the *target* or *core*, and one considers states for the total system with spin, orbital angular momentum and parity quantum numbers $SL\pi$. \mathcal{A} is an antisymmetrisation operator; χ_i is a vector-coupled product of a target eigenfunction times functions for the spin and angle coordinates for the electron; $F_i(r)$ is a radial function of the added electron and Φ_j is a bound-state type function for the entire system introduced to compensate for orthogonality conditions imposed on $F_i(r)$. The electron radial functions $F_i(r)$ and the coefficients c_j are treated as variational parameters leading to a set of coupled integro-differential equations which are solved numerically.

The accuracy of the CC method is comparable to that obtained by the best methods which have been developed to study, usually separately, b-b and b-f transitions. It is limited by the accuracy of the target eigenfunctions and the number of terms (channels) in the CC expansion. Considerable effort is concentrated in obtaining accurate target representations using configuration interaction codes such as SUPERSTRUCTURE (Eissner *et al* 1974) and CIV3 (Hibbert 1975).

5.2. The R -matrix method

In the OP the integro-differential equations of the CC approximation are solved by the *R-matrix method* (Burke *et al* 1971). In this method the configuration space is divided up into an inner region, where all detailed short-range electronic interactions are explicitly included, and an outer or asymptotic region where only long-range interactions are important. The boundary of the inner region, $r = a$, is chosen where the target wave functions have died down.

Solutions in the inner region are obtained by imposing a boundary condition at $r = a$, and this implies that the solutions, $\Psi = \psi_n$, will only exist for a discrete set of energies, $E = e_n$. These “unphysical states” are referred to as the *R-matrix states*. The boundary condition is usually taken to be

$$\frac{d}{dr} f_{in}(r)|_{r=a} = 0, \quad (12)$$

where $F_i(r) = f_{in}(r)$ are the radial part of ψ_n . The wave function Ψ_E (with radial part $F_{iE}(r)$) at any energy E can be expanded in terms of the *R-matrix states* by

$$\Psi_E = \sum_n \psi_n A_{nE}. \quad (13)$$

The expansion coefficients are obtained by diagonalising the Hamiltonian for the total system and can be expressed as

$$A_{nE} = (e_n - E)^{-1} \sum_i f_{in}(a) \frac{d}{dr} F_{iE}(r)|_{r=a}. \quad (14)$$

It may be shown that the radial functions $F_{iE}(r)$ at the boundary radius are given by

$$F_{iE}(a) = \sum_{i'} R_{ii'}(E) \frac{d}{dr} F_{i'E}(r)|_{r=a}, \quad (15)$$

where

$$R_{ii'}(E) = \sum_n f_{in}(a) (e_n - E)^{-1} f_{i'n}(a) \quad (16)$$

is the *R matrix*.

“Physical states” are obtained by matching solutions in the outer and inner regions at $r = a$ using expression (15). The attractive feature of the *R-matrix* method is that only one diagonalisation is required for each $SL\pi$ symmetry to obtain the *R-matrix* eigenfunctions at the boundary, $\{f_{in}(a)\}$, and its eigenvalues, e_n , and thus obtain, through the matching, the solution $\Psi_E^{SL\pi}$ at any energy. Recent innovative developments in the treatment of the asymptotic region (Berrington *et al* 1987) have dramatically enhanced the efficiency of the *R-matrix* method, particularly in the computation of bound states and radiative data.

5.3. Equation of state (EOS)

The EOS plays a central role in opacity calculations since it should model the thermodynamic environment where radiative processes take place and result in the optical characteristics of the plasma. In accord with the OP approach that ions exist as identifiable entities in stellar envelopes, a suitable EOS must then predict the distribution of ionisation and excitation states of the atomic species present in the plasma. In the OP radiative properties are calculated for isolated ions; however, plasma interactions cause important modifications, an outstanding effect being that the number of excited bound states of an ion will be thermodynamically dependent. That is, as the ion becomes more excited the mean ionic radius will eventually be larger than the distances to neighbouring particles, and the state can no longer be identified as a “true” bound state belonging to original ion. This problem can be appreciated in the Boltzmann population for a state i of ion j of species k given by

$$N_{ijk}/N_{jk} = g_{ijk} \exp(-E_{ijk}/kT)/Z_{jk} \quad (17)$$

where g_{ijk} is the statistical weight of the state and Z_{jk} is the *internal partition function* defined as

$$Z_{jk} = \sum_i g_{ijk} \exp(-E_{ijk}/kT). \quad (18)$$

For an isolated ion, with an infinite number of bound states, the summation in equation (18) is divergent whilst plasma interactions lead to a finite partition function.

Key problems inherent to the EOS, in particular the truncation of the partition function, have been discussed in detail in the series “Equation of state for stellar envelopes” (Hummer and Mihalas 1988 and papers thereafter), and a new EOS has been proposed which accounts for non-ideal effects. These authors have shown that the partition function may be sensitive to the theory behind the sum truncation, and that abrupt cutoffs can produce unwanted discontinuities in the thermodynamic and optical properties of the gas. They introduce a modified partition function

$$\tilde{Z}_{jk} = \sum_i w_{ijk} g_{ijk} \exp(-E_{ijk}/kT), \quad (19)$$

where w_{ijk} is now an occupation probability. These occupation probability factors are determined by the interactions with both neutral and charged perturbers, in particular by the ion micro-field. This formalism has definite advantages: it provides a smooth transition from bound to free states, and therefore assures continuity not only of the internal partition functions but also of all material properties; the occupation probabilities can be included into the free energy of the plasma in a statistically consistent way, and through a free-energy minimisation procedure a thermodynamically consistent EOS is derived.

5.4. Line broadening

Broadening of both lines and autoionisation resonances is of vital importance in the calculation of the RMO. Broadening is due to perturbations by both ions and electrons in the plasma. Ions, being heavier than electrons, can be regarded at rest and thus produce a mean electric field which perturbs the energy levels by the *Stark effect*. This contribution is particularly important for hydrogenic ions for which the Stark effect is linear. Electron collisional broadening can be satisfactorily treated within the CC approximation but only for a limited amount of transitions. Due to the large number of transitions that are being computed, empirical formulae must be employed (Seaton 1987b, 1988, 1989). A further interesting point is that it has been estimated that in general the line broadening will be larger than the fine-structure separations; consequently, calculations will be carried assuming LS coupling and neglecting relativistic effects.

VI. SELECTED RESULTS

In this section we have chosen the Mg isoelectronic sequence as a show-case of the atomic data that are being generated in the OP. The following ions were considered: Mg I, Al II, Si III, S V, Ar VII, Ca IX and Fe XV. We shall discuss the target representations employed, the bound states that are generated and the radiative transitions (b-b and b-f) involving them. These ions have previously received a great deal of attention from both experimentalists and theoreticians, and thus useful statistical comparisons between datasets can be made. The comparison between two datasets, $\{x\}$ and $\{x'\}$ say, will be carried out in terms of an *average percentage difference* defined as

$$\Delta(\{x\}, \{x'\}) = 100 \times \left[\sum_i (x_i - x'_i)^2 \right]^{1/2} \left[\sum_i x_i \times x'_i \right]^{-1/2}. \quad (20)$$

Work for this sequence within the OP was carried out by Keith Butler (Univ. Munich), Claude Zeippen (Obs. Paris) and myself.

6.1. Target representations

The Na-like cores were represented by a seven-state approximation: $3s$, $3p$, $3d$, $4s$, $4p$, $4d$ and $4f$. In the case of Mg II the $5s$ state was also included. Orbitals were calculated in a similar fashion to Butler *et al* (1984). These core representations should accurately reproduce the correlation effects of the two valence electrons of the core + electron system, in particular the double excitations which cause conspicuous series perturbations and resonances.

6.2. Bound states

Assuming a closed $2p^6$ shell, Mg-like ions ($Z \leq 26$) have bound states with electronic configurations $3lnl' m L\pi$, giving rise to spectroscopic series of singlet ($m = 1$) and triplet ($m = 3$) states of even or odd parity (π). In the present work bound states are calculated such that the principal quantum number of the main active electron is limited to the range $n \leq 10$, and the orbital angular momenta take the values $l \leq 2$, $l' \leq 4$ and $L \leq 4$. This gives rise to a total of 1247 bound states for the ions considered. A careful search of available spectroscopic measurements yielded only 374 observed multiplets. A sensitive comparison with experiment can be carried out in terms of the *quantum defect*, μ_n , defined by the expression

$$E_n = E_\infty - z^2 / (n - \mu_n)^2, \quad (21)$$

where E_n is the energy of the state in Rydberg units, E_∞ is the energy of the corresponding spectroscopic series limit and z is the effective charge of the ion. The quantum defect gives a measure of the departure of a state from its hydrogenic energy position. The comparison with the OP results gives an average percentage difference of $\Delta(\{\mu_{op}\}, \{\mu_{expt}\}) = 2.4\%$, if 6 states with questionable experimental assignments are excluded: $3p4p^1D$ and

$3s7d\ ^1D$ of Si III; $3p3d\ ^1P^0$ and $3p3d\ ^1F^0$ of S V; $3s5f\ ^1F^0$ and $3s6f\ ^1F^0$ of Fe XV. Two conclusions emerge from this comparison. Firstly, the number of states in relation with spectroscopic data has been increased by a factor of 3 and, secondly, the theoretical multiplet energies are statistically of high accuracy.

6.3. Oscillator strengths and radiative lifetimes

The contribution to the monochromatic opacity from a b-b transition takes the form

$$\kappa_\nu(i \rightarrow j) = N_i \frac{2\pi^2 e^2}{mc} f_{ij} \phi_i(\nu), \quad (22)$$

where N_i is the population of the initial state, $\phi_i(\nu)$ is the line profile and f_{ij} is the absorption *oscillator strength* (f-value). In the OP, f-values are calculated for all optically allowed transitions. Experimentalists usually measure radiative lifetimes; the *lifetime* of a state is defined as

$$\tau_j = \left(\sum_i A_{ji} \right)^{-1}, \quad (23)$$

where A_{ji} is the spontaneous decay *transition probability*. The latter can be expressed in terms of the f-value by the relation

$$A_{ji} = \frac{\alpha^3 E_{ij}^2}{2\tau_0} \frac{g_i}{g_j} f_{ij}. \quad (24)$$

α is the fine structure constant, τ_0 is the atomic time unit, E_{ij} is the photon energy in Rydberg units and g_i and g_j are statistical weights.

The 1247 bound states give rise to 17041 possible transitions. In order to get an estimate of the accuracy of the computed f-values, we compare the present dataset in Table 1 with four sets of independent calculations which we believe are representative of previous work on Mg-like ions. In this comparison we have excluded four transitions from set MCHF involving the heavily mixed $3p3d\ ^1P^0$ and $3s6p\ ^1P^0$ states of Si III, since radiative properties for states where strong mixing is present are very difficult to obtain with some reliability. Likewise we have excluded from set CIV3 two transitions involving the $3p4p\ ^1D$ and $3s5d\ ^1D$ states of S V. Set MS only includes radiative data for Mg I and therefore the agreement is not representative of the whole sequence. We conclude that the present f-value dataset is of comparable or better statistical accuracy than previous theoretical work, and the number of quoted transitions has been greatly enlarged.

In the present work radiative lifetimes can be computed for all the bound states considered. This is an improvement over several previous calculations where for some transitions only upper bounds are given due to the neglect of decay channels. We find good agreement (better than 15 %) with the lifetimes recently calculated by Moccia and Spizzo (1988) for 25 states of Mg I. Similarly, differences with the lifetimes computed for 57 singlet states of ions of the this sequence by Froese Fischer and Godefroid (1982) are not larger than 20 %, if one excludes the long-lived $3p^2\ ^1D$ state of Al II and the strongly mixed $3p3d\ ^1P^0$ and $3s6p\ ^1P^0$ of Si III. Better agreement would perhaps be attained if the lifetimes were calculated using experimental photon energies (equations 23 and 24). On the other hand, the comparison with experimental results does not lead to an overall conclusion. Lifetimes for Mg-like ions have been measured by a large number of research groups, and there is a wide scatter in the agreement between different sets of experimental results.

Table 1. Comparison of f-value (length formulation) average percentage differences between present results and representative sets of values calculated previously for ions in the Mg sequence. VSL: Model potential method of Victor *et al* (1976). MCHF: Multiconfiguration Hartree-Fock results of Froese Fischer (1975, 1979) and Froese Fischer and Godefroid (1982). CIV3: Configuration interaction calculations by Bahuja and Hibbert (1980, 1985), Tayal and Hibbert (1984) and Tayal (1986). MS: L^2 method of Moccia and Spizzo (1988).

Set	No. Trans.	$\Delta(\{f_{op}\}, \{f_{set}\})$ (%)
VSL	615	8.3
MCHF	219	2.2
CIV3	337	4.8
MS	429	1.9

6.4. Photoionisation cross sections

When a bound state is photoionised (i.e., a b-f transition) the resulting monochromatic opacity is given by

$$\kappa_{\nu}(i) = N_i \sigma_{\nu}(i) \phi_p(\nu), \quad (25)$$

where $\sigma_{\nu}(i)$ is the photoionisation cross section of the state and $\phi_p(\nu)$ is a normalised profile. In the OP, total photoionisation cross sections are calculated for all bound states, tabulated in meshes fine enough to resolve the resonances.

In fig. 3 we show the photoionisation cross sections of the $3sns \ ^1S$ ($n \leq 5$) bound states of Al II. The cross sections are dominated below the Al III $3p \ ^2P^0$ threshold ($E \simeq 0.49$ Ryd) by a series of window resonances due to transitions of the type

$$3sns \ ^1S + \hbar\omega \rightarrow 3pn's \ ^1P^0 \rightarrow 3s \ ^2S + e. \quad (26)$$

For instance, the $3p4s \ ^1P^0$ resonance causes the cross section of the $3s^2 \ ^1S$ ground state (Fig. 3a) to be very small at the reaction threshold ($E = 0.0$ Ryd). Furthermore, a significant behaviour has emerged from the study of photoionisation of excited states, namely that due to resonances arising from only photoexcitation of the core, that is, for cases where $n = n'$ in equation (26). The effect caused by these resonances, referred to as *PEC resonances* (Yu Yan and Seaton 1987), may be appreciated in the cross sections of the $3s4s \ ^1S$ and $3s5s \ ^1S$ excited states of Al II (Figs. 3b and 3c), where the $3p4s \ ^1P^0$ and $3p5s \ ^1P^0$ resonances, respectively, switch from deep windows to broad peaks almost two orders of magnitude higher than the background cross sections. PEC resonances will be of considerable importance in the continuum contribution to the RMO.

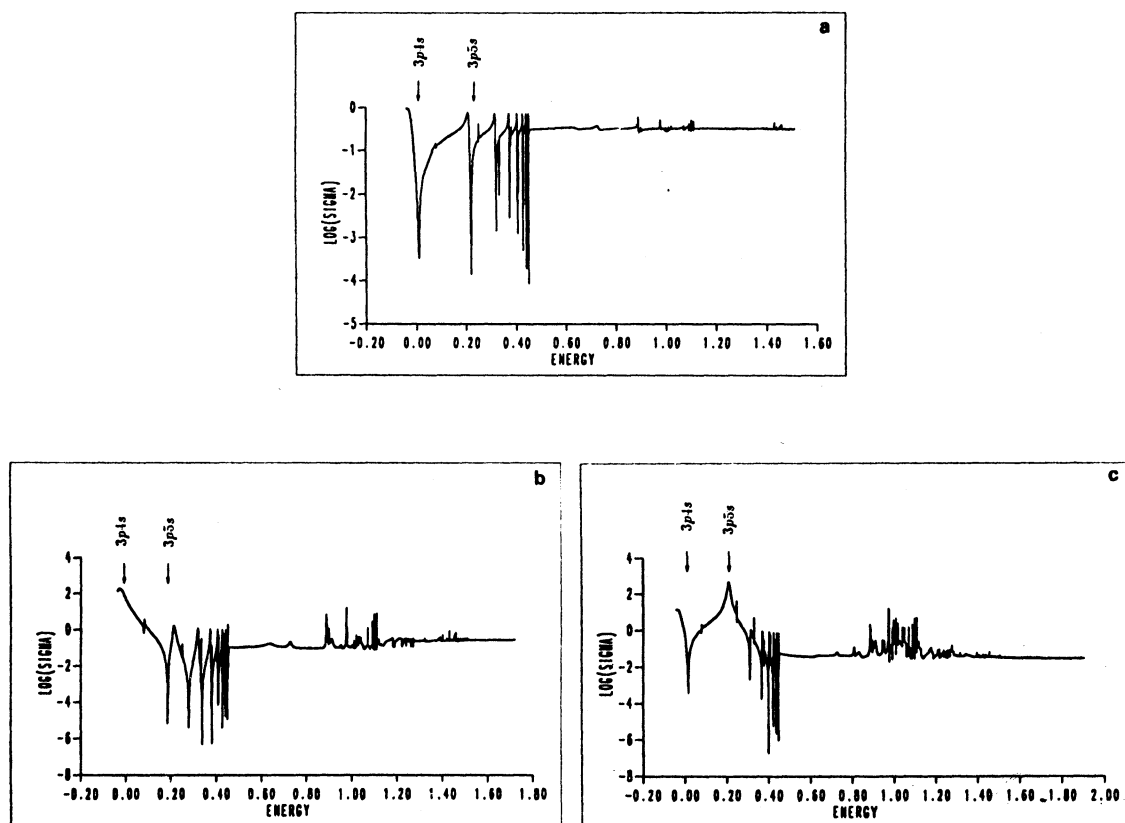


Figure 3. Photoionisation cross sections (Mb) of the $3sns \ ^1S$ states of Al II plotted as a function of photoelectron energy (Ryd). a) $3s^2$. b) $3s4s$. c) $3s5s$.

ACKNOWLEDGEMENTS

I am deeply grateful to all participants of the OP for enjoyable and fruitful team work, specially to Professor M.J. Seaton as project leader. My participation in the project has been fully supported by IBM Venezuela for which I am indebted. Part of the work for this talk was carried out during a visit to the Observatoire de Paris, Meudon, in July 1989; financial support from the Observatoire is kindly acknowledged. I would like to thank Claude Zeippen for the invitation and for useful discussions regarding the content of this paper. Finally, I appreciate comments on the actual presentation of the talk by Helaine Barroso dos Reis from the Observatório Nacional in Rio.

REFERENCES

- Balona, L.A. 1985, in *Cepheids: Theory and Observations*, ed. B.F. Madore (Cambridge: Cambridge University Press), p. 17.
- Baluja, K.L., and Hibbert, A. 1980, *J. Phys. B*, **13**, L327.
- Baluja, K.L., and Hibbert, A. 1985, *Nucl. Instr. Meth.*, **B9**, 477.
- Becker, S.A. 1985, in *Cepheids: Theory and Observations*, ed. B.F. Madore (Cambridge: Cambridge University Press), p. 104.
- Becker, S.A. 1987, in *Stellar Pulsation*, eds. A.N. Cox, W.M. Sparks, S.G. Starrfield (Berlin: Springer-Verlag), p. 16.
- Berrington, K.A., Burke, P.G., Butler, K., Seaton, M.J., Storey, P.J., Taylor, K.T., and Yu Yan. 1987, *J. Phys. B*, **20**, 6379 (ADOC II).
- Bertelli, G., Bressan, A.G., and Chiosi, C. 1984, *Astron. Astrophys.*, **130**, 279.
- Burke, P.G., Hibbert, A., and Robb, W.D. 1971, *J. Phys. B*, **4**, 153.
- Burke, P.G., and Seaton, M.J. 1971, *Meth. Comput. Phys.*, **10**, 1.
- Butler, K., Mendoza, C., and Zeippen, C.J. 1984, *M.N.R.A.S.*, **209**, 343.
- Carson, T.R. 1976, *Ann. Rev. Astron. Astrophys.*, **14**, 95.
- Carson, T.R., and Hollingsworth, H.M. 1968, *M.N.R.A.S.*, **141**, 77.
- Carson, T.R., Huebner, W.F., Magee, N.H., and Merts, A.L. 1984, *Ap. J.*, **283**, 466.
- Carson, T.R., Mayers, D.F., Stibbs, D.W.N. 1968, *M.N.R.A.S.*, **140**, 483.
- Carson, T.R., and Stothers, R.B. 1984, *Ap. J.*, **276**, 593.
- Carson, T.R., Stothers, R.B., and Vemury, S.K. 1981, *Ap. J.*, **244**, 230.
- Cox, A.N. 1965, in *Stars and Stellar Systems*, Vol. 8: *Stellar Structure*, eds. L.H. Aller and D.B. McLaughlin (Chicago: University of Chicago Press), p. 195.
- Cox, A.N. 1980, *Ann. Rev. Astron. Astrophys.*, **18**, 15.
- Cox, A.N., and Stewart, J.N. 1965, *Ap. J. Suppl. Ser.*, **11**, 22.
- Cox, A.N., and Stewart, J.N. 1970a, *Ap. J. Suppl. Ser.*, **19**, 243; 1970b, **19**, 261.
- Cox, A.N., Stewart, J.N., and Eilers, D.D. 1965, *Ap. J. Suppl. Ser.*, **11**, 1.
- Cox, A.N., and Tabor, J.E. 1976, *Ap. J. Suppl. Ser.*, **31**, 271.
- Cox, J.P. 1985, in *Cepheids: Theory and Observations*, ed. B.F. Madore (Cambridge: Cambridge University Press), p. 126.
- Eissner, W., Jones, M., and Nussbaumer, H. 1974, *Comput. Phys. Commun.*, **8**, 270.
- Feast, M.W., and Walker, A.R. 1987, *Ann. Rev. Astron. Astrophys.*, **25**, 345.
- Fricke, K., Stobie, R.S., and Strittmatter, P.A. 1971, *M.N.R.A.S.*, **154**, 23.
- Froese Fischer, C. 1975, *Can. J. Phys.*, **53**, 184.
- Froese Fischer, C. 1979, *J.O.S.A.*, **69**, 118.
- Froese Fischer, C., and Godefroid, M. 1982, *Nucl. Instr. Meth.*, **202**, 307.
- Hibbert, A. 1975, *Comput. Phys. Commun.*, **9**, 141.
- Huebner, W.F. 1986, in *Physics of the Sun*, Vol. 1, ed. P.A. Sturrock (Dordrecht: Reidel), p. 33.
- Hummer, D.G., and Mihalas, D. 1988, *Ap. J.*, **331**, 794 (EOS I).
- Iben, I. 1974, in *Stellar Instability and Evolution*, eds. P. Ledoux, A. Noels and A.W. Rogers (Dordrecht: Reidel), p. 3.
- Iglesias, C.A., Rogers, F.J., and Wilson, B.G. 1987, *Ap. J.*, **322**, L45.
- Magee, N.H., Merts, A.L., and Huebner, W.F. 1975, *Ap. J.*, **196**, 617.
- Magee, N.H., Merts, A.L., and Huebner, W.F. 1984, *Ap. J.*, **283**, 264.
- Mihalas, D. 1978, *Stellar Atmospheres* (San Francisco: Freeman).
- Moccia, R., and Spizzo, P. 1988, *J. Phys. B*, **21**, 1133.
- Pradhan, A.K. 1987, *Physica Scripta*, **35**, 840.
- Seaton, M.J. 1987a, *J. Phys. B*, **20**, 6363 (ADOC I); 1987b, **20**, 6431 (ADOC V).
- Seaton, M.J. 1988, *J. Phys. B*, **21**, 3033 (ADOC VIII).

- Seaton, M.J. 1989, *J. Phys. B*, **22**, 3603 (ADOC XII).
- Simon, N.R. 1982, *Ap. J.*, **260**, L87.
- Simon, N.R. 1987, in *Stellar Pulsation*, eds. A.N. Cox, W.M. Sparks, S.G. Starrfield (Berlin: Springer-Verlag), p. 148.
- Schmidt, E. 1984, *Ap. J.*, **285**, 501.
- Stellingwerf, R.F. 1978, *A. J.*, **83**, 1184.
- Tayal, S.S. 1986, *J. Phys. B*, **19**, 3421.
- Tayal, S.S., and Hibbert, A. 1984, *J. Phys. B*, **17**, 3835.
- Temury, S.K., and Stothers, R. 1978, *Ap. J.*, **225**, 939.
- Tector, G.A., Stewart, R.F., and Laughlin, C. 1976, *Ap. J. Suppl. Ser.*, **31**, 327.
- Tu Yan and Seaton, M.J. 1987, *J. Phys. B*, **20**, 6409 (ADOC IV).

Claudio Mendoza: IBM Venezuela Scientific Center, Apdo. 64778, Caracas 1060A, Venezuela.